Simulation Of The Hydrodynamic Interaction of Bodies

by

Hua-Yang Wu

Submitted to the Department of Ocean Engineering
in partial fulfillment of the requirements for the degree of

Master of Science in Naval Architecture and Marine Engineering

at the

MASSACHUSETTS INSTITUTE OF TECHNOLOGY

February 1995

Author . . . .
Department of Ocean Engineering
January 20, 1995

Certified by . . . .
F. Thomas Korsmeyer
Lecturer
Thesis Supervisor

Accepted by . . . .
A. Douglas Carmichael
Chairman, Departmental Committee on Graduate Students

Simulation Of The Hydrodynamic Interaction of Bodies

by

Hua-Yang Wu

Abstract

When two ships are operating in proximity, the resulting hydrodynamic forces can cause significant loads on the ships. Such problems can be solved by a numerical approach, based on the use of a three-dimensional panel method. The objective of this paper is to compute the case of two ships which are allowed to move under the influence of the hydrodynamic forces. In this problem, the direct evaluation of the time derivative term from Bernoulli's equation may be computed by one-sided finite difference if two ships are moving. A new approach presented here is to partially combine Bernoulli's equation and Lagrange's equation. Numerical experiments will demonstrate and validate the efficacy of this approach from the concept of the "possible displacement" which leads to a more accurate two-sided finite difference scheme.

Acknowledgments

I am particularly grateful to my advisor, F. Thomas Korsmeyer for his patience, encouragement and guidance. Also, I would like to express my appreciation to my friends for their warm care. Finally, this thesis is dedicated to my parents for their love and support.

Contents

List of Figures

Chapter 1

Introduction

Hydrodynamic interaction forces become an important consideration in restricted waters such as ports or channels because ships are operating near to each other due to navigational constraints. Therefore it is necessary to build a model for predicting the relative positions of the bodies which may be ships or ocean structures under the influence of hydrodynamic forces.

Most studies of interaction forces between bodies are restricted in the cases of two bodies of simple geometries with known velocities, such as two bodies passing each other in opposite directions with steady-state velocities or one body passing a stationary one. The present study is an extension of Korsmeyer *et al.* (1993) [5] in which geometrical idealizations are removed by adopting a three-dimensional panel method. The condition of steady-steady velocities is relaxed in the present study which allows the bodies to be moved by the hydrodynamic forces, but the method is still applied to cases with steady-state velocities for validation.

Some experimental studies have been surveyed in this field. Cohen and Beck (1983) [1] have tested the interaction forces of a mathematical hull form passing another stationary mathematical shape in shallow water with the presence of rectangular channels.

Some computations have been made by Landweber, Chwang & Guo (1991) [7]. In their paper, Lagrange's equation is used to predict the hydrodynamic forces. They consider the case of one body stationary and the other approaching it along a line

joining bodies' centroids. If the bodies are laterally symmetrical, there is only one degree of freedom for each body, because it can be expected that there is no sway force and yaw moment acting on the bodies. Under such a simplification, they are able to solve the equation of motion in closed-form, in terms of the added-mass coefficients, and obtain simple expressions for the velocity of the moving body as a function of its relative position. Isaacson and Cheung (1988) [3] consider the case of one body drifting in an incident wave near another one. They approach the two-body problem in two dimensions from the pressure distribution given by Bernoulli's equation, although their method can be extended to three dimensions. In their paper, the velocity potential is decomposed into a component associated with an incident wave potential, a diffraction potential, and a potential due to the motion of the moving body. However, Landweber *et al.* (1991) [7] pointed out that there are some missed terms related the derivatives of the unit potentials in their force expression due to an incorrect assumption that " unit potentials are invariant with time ..." Actually, the unit potential is a function of the geometrical configuration of the bodies and any enclosing boundaries which may vary with time. Therefore the derivatives of the unit potentials can not be disregarded in the force expressions.

If Lagrange's equation is used for the case of bodies influenced by the hydrodynamic forces, it is not superior to the approach from Bernoulli's equation. In Lagrange's equation, for every single related modes the spatial derivative may be done numerically by moving the body back and forth from the exact position. This definitely increases much computational burden because in the present study the bodies are free to move in different modes under the influence of the hydrodynamic forces. The advantages of Lagrange's equation are that the evaluations of the fluid velocities are avoided, and the spatial derivatives can be calculated by two-sided finite difference.

For computational convenience, the partial derivative with respect to time of the velocity potential in Bernoulli's equation can be replaced by the total derivative with respect to time minus a convective derivative (or a "transport" term). If the bodies' velocities are known a priori, then this total derivative may be calculated to

any desired accuracy by shortening the time interval and applying some numerical differentiation technique. However, if the body positions are influenced by the hydrodynamic forces, the following relative position is unknown before getting the forces at the current time instant. The exception is in some simplified case like [7] in which the equation of motion can be solved in a closed form. For more complicated cases, there is no closed-form solution of the relative positions. Therefore, the direct evaluation of the total derivative may only be done by one-sided finite difference, because all known information is previous to the current time instant.

In the present study, the time derivative is split into two terms. One of them contains the unknown accelerations, and the other is calculated by two-sided finite difference from the concept of the "possible displacement" which is different from the actual displacement. That altered force expression can be combined with the equation of motion in order to eliminate the unknown hydrodynamic forces, and finally form a linear system for the unknown accelerations. After obtaining the accelerations, the hydrodynamic forces and the relative position of the next time instant can be calculated. Since the altered expression for the hydrodynamic forces makes the calculations of the time derivative by two-sided finite difference possible, there is a consequent decrease in the computational work for a given accuracy.

The flow problems are formulated under two major assumptions:

1. Ideal flow is assumed, without viscous effects.

2. Free-surface effects are ignored.

The integral equations are discretized as a linear system by a panel method. The panel method approach, which follows from the pioneering work of Hess and Smith (1962) [2], is to represent the geometry of the problem by quadrilateral or triangular panels and assume the strengths of the singularities to be unknown constants over the panels.

The present study is an extension of the program CHANEL, a derivative of the program WAMIT (Wave Analysis MIT). The program CHANEL is a panel-method program which computes the hydrodynamic forces for the case of one body fixed and

one body in translation with constant velocity. There are no assumptions about the form of the bodies or their relative positions. The extended version implements the features of allowing two bodies to be moved by the hydrodynamic forces, and utilizing the altered expression outlined above.

Three different methods are described in §2 for computing the force and moment on each body, presuming the velocity potential and source strength have been determined on the surface of the body. The mathematical formulations for the flow problems are outlined in §3. The influence of the propeller on the hydrodynamic force is surveyed in §4. Numerical techniques are discussed in §5. Computational results are presented in §6 for validation and efficacy. Conclusions and possible extensions are included in §7.

Chapter 2

Force Expressions

2.1 Bernoulli's Equation

In this section, we show how the hydrodynamic forces and moments are obtained by Bernoulli's equation. Presume that the flow problem can be solved without difficulty, so the hydrodynamic forces and moments acting on each body may be evaluated by integration of the pressure over the corresponding wetted surface. We consider two general three-dimensional bodies floating on a free surface and undergoing arbitrary six-degree-of-freedom motion. Thus, the generalized coordinates x_i are defined as the displacements of each of the bodies in each mode of motion. That is, x_1 through x_6 denote the displacements for six degrees of freedom for the first body, x_7 through x_{12} denote the displacements for the second body. Therefore, the configuration of this two-body dynamic system can be described completely by those generalized coordinates. The position vector $\vec{x} \equiv \{ x_i \}$ is a function of time and the corresponding bodies' velocities are $u_i = \dot{x}_i$, where the dot denotes time differentiation. The generalized normal vector is n_i, and is defined similarly. Integrating the pressure from Bernoulli's equation over the body's surface we obtain the expression for the forces and moments,

$$F_i = -\rho \int \int_{S_B} (\frac{\partial \phi}{\partial t} + \frac{1}{2}\nabla \phi \cdot \nabla \phi) n_i dS, \qquad (2.1)$$

where S_B denotes the union of the bodies' wetted surface, since n_i is nonzero only on the body for which the mode i is defined. In (2.1), the partial derivative with respect to time of the velocity potential, which is also called the local derivative, represents the rate of change of the velocity potential with respect to time at a fixed position. Because numerically the velocity potential is evaluated on the bodies' surfaces, it is awkward to directly evaluate the partial derivative if the body is moving. The partial derivative may be evaluated by

$$\frac{d\phi}{dt} = \frac{\partial\phi}{\partial t} + (\vec{U} \cdot \nabla\phi), \tag{2.2}$$

where the vector $\vec{U}$ contains the corresponding bodies' velocities. The total derivative, $d\phi/dt$, represents the rate of the change of the velocity potential with respect to time in a coordinate system moving with the element which we are interested in. In other words, The value of $d\phi/dt$ is obtained by following the motion of an element of fixed identity and calculating the difference of the velocity potential at different time instants. The second term on the right hand side is called the convective derivative because it represents the change of the velocity potential caused by the convection of an element from one position to a second position having a different value of the velocity potential. Since (2.2) is correct for every particle on the surfaces, after integration over the surface S_B (2.2) becomes

$$\rho\frac{d}{dt}\int\int_{S_B}\phi n_i dS = \rho\int\int_{S_B}(\frac{\partial\phi}{\partial t})n_i dS + \rho\int\int_{S_B}(\vec{U}\cdot\nabla\phi)n_i dS. \tag{2.3}$$

Since the time-derivative and surface integration are independent, these operators can be interchanged. Substituting (2.3) into (2.1) leads to a force expression,

$$F_i = -\rho\frac{d}{dt}\int\int_{S_B}\phi n_i dS + \rho\int\int_{S_B}((\vec{U}\cdot\nabla\phi)n_i - \frac{1}{2}\nabla\phi\cdot\nabla\phi n_i)dS. \tag{2.4}$$

An alternative expression for the forces may be derived from the transport theorem

as is shown in Newman (1977 §4.12) [9]:

$$\rho\frac{d}{dt}\int\int_{S_B}\phi n_i dS = \rho\int\int_{S_B}(\frac{\partial\phi}{\partial t})n_i dS + \rho\int\int_{S_B}(\frac{\partial\phi}{\partial n}V_i)dS. \qquad (2.5)$$

Here V_i is defined respectively as the i-th component of the fluid velocity vector $\nabla\phi$ or the cross-product $r \times \nabla\phi$, evaluated on the body corresponding to mode i and elsewhere on S_B $V_i = 0$. The second integral on the right hand side represents the transport of the quantity of V_i out of the volume $\mathcal{V}$, as a result of the movement of the boundary. Adding (2.1) and (2.5) together, we obtain another force expression.

$$F_i = -\rho\frac{d}{dt}\int\int_{S_B}\phi n_i dS + \rho\int\int_{S_B}(\frac{\partial\phi}{\partial n}V_i - \frac{1}{2}\nabla\phi\cdot\nabla\phi n_i)dS. \qquad (2.6)$$

Both (2.4) and (2.6) are valid. The only difference between two equations is the "convective derivative" term and the "transport" term. A comparison of the numerical results of both terms will be show in §6. Hereafter, (2.6) is employed in the present study.

The first integral in (2.6) is the added-mass. For a single body, moving with constant velocities in an unbounded flow, this integral is independent of the body's position when expressed in terms of a coordinate system moving with the body. When other boundaries are present, including both a channel and a second body, this integral will depend on the configuration of the system and the bodies' velocities. Thus at different time instants this quantity will change, and the resulting time derivative indicated in (2.6) is the "linearized" force or moment acting on the respective body. The second integral in or (2.6) represents an additive "quadratic" component to each force and moment. If the bodies are moved by the hydrodynamic forces, the direct evaluation of the time derivative term of (2.6) may only be done numerically by one-sided finite difference, because the positions of bodies at the next time-step are not known before the forces are computed.

2.2 Lagrange's Equation

A different approach for hydrodynamic forces is established by Milne-Thomson. The cardinal idea of this method is that the bodies and the fluid are treated as forming together one dynamical system, and thus the troublesome calculation of the effect of the fluid pressure on the surface of the body is avoided.

The following is mainly from Milne-Thomson (1960, §17.60) [8] and Lamb (1932, §6) [6]. To begin with this approach, first consider a single body immersed in an unbounded fluid. If the body is moving, the resulting motion of the fluid will be irrotational and acyclic. The irrotationality is due to the consequence of Kelvin's theorem, and the acyclic is explained by the following statement. If the bodies are moved through a cycle of positions and returned to their own original positions, there is no evidence that the fluid particles are each in their original positions. Moreover, such a motion once established will instantly cease if the body stops moving. We will suppose that the motion of the fluid is entirely due to the motion of the body.

Under such circumstances, the motion of the fluid is determined by the existence of a velocity potential ϕ which must satisfy the Laplace equation and the boundary conditions. If the single body is replaced by a group of bodies, this argument still holds.

If there are n degrees of freedom in a dynamical system, n independent coordinates are necessary to describe the motion of the system, and these are called the generalized coordinates. Therefore, we can conceive that the position of any specified dynamical system is determinable in terms of a certain number of generalized coordinates $x_1, x_2, ..., x_n$.

When bodies and fluid are formed together as a dynamical system, the generalized coordinates serve to specify the configuration of the bodies. In other words, a n-dimensional configuration space is built by n generalized coordinates, and the configuration of the system at an arbitrary instant is a point in the configuration space. Therefore the motion of the dynamic system can be "visualized" as a curve in the configuration space. The fluid, however, has infinite freedom which can not be

13

described by a finite number of the generalized coordinates, i.e. the positions of the various particles of the fluid are not determined by the instantaneous values of the coordinates of the bodies. However, the boundary condition still holds

$$\frac{\partial \phi}{\partial n} = V_n, \tag{2.7}$$

where V_n is the normal component of the velocity of the fluid. But by hypothesis, V_n is a linear function of the generalized velocities $u_1, u_2, ..., u_n$, so that the boundary condition (2.7) together with the Laplace equation determine ϕ uniquely as a linear function of the generalized velocities. Therefore the total velocity potential can be expressed as the sum

$$\phi = u_i \phi_i, \tag{2.8}$$

in which ϕ_i represents the velocity potential due to a body motion with unit velocity in the i-th mode. The unit velocity potential, ϕ_i, also satisfies the Laplace equation, and is a function of the geometrical configuration of the bodies and any enclosing boundaries, but not of the velocities.

Under such a consideration, Milne-Thomson(1960, §17.60) [8] was able to derive a force expression by Lagrangian mechanics with the result:

$$F_i = -\frac{d}{dt}\left(\frac{\partial T_L}{\partial u_i}\right) + \frac{\partial T_L}{\partial x_i}, \tag{2.9}$$

where T_L is the kinetic energy of the fluid. We may express (2.9) in terms of the added-mass coefficients. The added-mass coefficients is defined as

$$m_{ij} = \rho \int\int_{S_B} \phi_j n_i dS. \tag{2.10}$$

It should be noted that the added-mass coefficients are functions of the configuration of the system only, i.e. the generalized coordinates. Actually, the added-mass

14

coefficients may be expressed in another form

$$m_{ij} = \rho \int \int_{S_B} \phi_j n_i dS = \rho \int \int_{S_B} \phi_j \frac{\partial \phi_i}{\partial n_i} dS$$

$$= \rho \int \int_{S_B} \phi_j (\nabla \phi_i \cdot n) dS = \rho \int \int \int_{\mathcal{V}} \nabla \cdot (\phi_j \nabla \phi_i) d\mathcal{V}$$

$$= \rho \int \int \int_{\mathcal{V}} (\nabla \phi_j \cdot \nabla \phi_i) d\mathcal{V} + \rho \int \int \int_{\mathcal{V}} (\phi_j \cdot \nabla^2 \phi_i) d\mathcal{V}$$

$$= \rho \int \int \int_{\mathcal{V}} (\nabla \phi_j \cdot \nabla \phi_i) d\mathcal{V}, \qquad (2.11)$$

where the divergence theorem and Laplace equation have been used, and the volume integrals are over the entire fluid volume. It is clear that the added-mass coefficients are symmetrical from (2.11). Therefore, we can express the kinetic energy of the fluid in terms of the added-mass coefficients

$$T_L = \frac{1}{2} \rho \int \int \int_{\mathcal{V}} VV d\mathcal{V} = \frac{1}{2} \rho \int \int \int_{\mathcal{V}} (\nabla \phi \cdot \nabla \phi) d\mathcal{V}$$

$$= \frac{1}{2} \rho \int \int \int_{\mathcal{V}} (u_i \nabla \phi_i) \cdot (u_j \nabla \phi_i) d\mathcal{V} = \frac{1}{2} u_i u_j \rho \int \int \int_{\mathcal{V}} (\nabla \phi_i \cdot \nabla \phi_j) d\mathcal{V}$$

$$= \frac{1}{2} u_i u_j m_{ij}, \qquad (2.12)$$

where (2.11) is used. It should be pointed out that the kinetic energy is a function of the generalized coordinates and their derivatives, the generalized velocities. Both the generalized coordinates and the generalized velocities are functions of time. Substituting (2.12) in (2.9), we can get

$$\frac{\partial T_L}{\partial x_i} = \frac{1}{2} u_j u_k \frac{\partial m_{jk}}{\partial x_i} \qquad (2.13)$$

$$\frac{\partial T_L}{\partial u_i} = \frac{1}{2} m_{ij} (u_k \delta_{ij} + u_j \delta_{ik}) = u_j m_{ij} \qquad (2.14)$$

$$\frac{d}{dt} \left(\frac{\partial T_L}{\partial u_i} \right) = m_{ij} \dot{u}_j + u_j u_k \frac{\partial m_{ij}}{\partial x_k}, \qquad (2.15)$$

where $\dot{u}_j$ denotes the acceleration in the j-th mode. Adding those results together,

15

(2.9) becomes

$$F_i = -m_{ij}\dot{u}_j - u_j u_k \left(\frac{\partial m_{ij}}{\partial x_k} - \frac{1}{2} \frac{\partial m_{jk}}{\partial x_i} \right)$$ (2.16)

This result has been shown by Korsmeyer, *et al.* (1993) [5].

The characteristic of the Lagrangian formulation is to express the force and moment strictly in terms of the added-mass coefficients, which avoids the evaluation of the velocity on the body surface. In (2.16), the spatial derivatives of the added-mass coefficients can be done numerically by two-sided finite difference. For every single related mode, the spatial derivative can be done by moving the body back and forth from the exact position, and calculating the difference of the added-mass coefficients. In our present case, where both bodies are moved by the hydrodynamic forces in surge, sway and yaw, the computational burden would be increased as much as one order of magnitude.

2.3   Combined Approach

After discussing Lagrange's equation and Bernoulli's equation, we can arrive at an alternative approach which takes advantage of both formulations. Compared to (2.6), the derivative terms of (2.16) can be calculated by two-sided finite difference, but require more computations because many modes need to be done separately. This alternative approach starts from expressing the first term in (2.6) in terms of the added-mass coefficients.

$$\rho\frac{d}{dt}\int\int_{S_B}\phi n_i dS = \rho\int\int_{S_B}\frac{d}{dt}(u_j\phi_j)n_i dS$$

$$= \rho\int\int_{S_B}\frac{du_j}{dt}\phi_j n_i dS + \rho u_j\int\int_{S_B}(\frac{d\phi_j}{dt})n_i dS$$

$$= \rho\dot{u}_j\int\int_{S_B}\phi_j n_i dS + \rho u_j\frac{d}{dt}\int\int_{S_B}\phi_j n_i dS$$

$$= \dot{u}_j m_{ij} + u_j\frac{dm_{ij}}{dt} \tag{2.17}$$

$$= \dot{u}_j m_{ij} + u_j\frac{\partial m_{ij}}{\partial x_k}\frac{dx_k}{dt} \tag{2.18}$$

$$= \dot{u}_j m_{ij} + u_j u_k\frac{\partial m_{ij}}{\partial x_k}. \tag{2.19}$$

From (2.19), it is clear that the first term in (2.6) is equal to the sum of the first two terms in (2.16). Numerically, the spatial derivatives in (2.19) can be done by two-sided finite difference. Observing the process from (2.18) to (2.19), the relation $dx_k/dt = u_k$ has been used. Therefore if we go one step backward and use the relation $d\vec{x}/dt = \vec{u}$ in (2.17), the time derivative of the added-mass coefficients can be done by two-sided finite difference. Substituting (2.17) in (2.6) yields

$$F_i = -m_{ij}\dot{u}_j - u_j\frac{dm_{ij}}{dt} + \rho\int\int_{S_B}(\frac{\partial\phi}{\partial n}V_i - \frac{1}{2}\nabla\phi\cdot\nabla\phi n_i)dS \tag{2.20}$$

The advantage of (2.20) is that we can use two-sided finite differencing to evaluate the time derivative in the second term with less computational work for a given

17

accuracy than with one-sided finite differencing. Numerically, the calculation of the second term in (2.20) is made via the concept of the "possible displacement" in which the generalized coordinates of the system are considered to be incremented by an infinitesimal amount from the values they have at an arbitrary instant. In (2.20), the infinitesimal increment which is the possible displacement, is computed by adopting the velocity at the arbitrary instant. By moving the bodies with the positive and negative orientations of the velocities at each time-step, we find two possible positions for each body. Of course, these positions are not actually on the paths of the bodies unless the velocities are steady. The time-derivative term in (2.20) may be computed by performing two-sided finite difference of the added-mass coefficients at the two possible positions.

For the possible displacement, it is appropriate to (2.17) that the velocities are maintained invariant. Observing (2.17), the time derivative has been split into two terms. One of them contains the unknown accelerations representing the rate of change of velocities with respect to time, and the other takes care of the rate of change of the added-mass coefficients with respect to time. In other words, for the second term on the right hand side of (2.17) we only consider the changes of the unit potentials which are due to the configuration only. The contributions from the changes of the velocities are relegated to the first term. At this point, it can be understood that this two-sided finite difference can not be applied to the left hand side of (2.17), because the contributions from the change of the velocities would be lost.

If we use R_i to denote the the last integral in (2.20), we can rewrite (2.20) as

$$F_i = -m_{ij}\dot{u}_j - u_j\frac{dm_{ij}}{dt} + R_i. \tag{2.21}$$

The next step is to write down the equations of motion. It is reasonable to ignore the motions in heave, roll and pitch which will be balanced by the hydrostatic restoring forces, because the major concern in the present study is the relative position of the two bodies in the horizontal plane. Therefore a 3x3 mass matrix is formed for

18

each body due to the previous simplification. Furthermore, if we assume that all the hydrodynamic forces and the external forces are referred to the center of gravity, all off-diagonal entries drop out in the mass matrix. Therefore the equations of motion can be reduced to

$$F_i + F_{ei} = m\dot{u}_i, \qquad (2.22)$$

where m denotes the mass or the moment inertia of the body in the i-th mode, and F_{ei} denotes the given external forces other than the hydrodynamic force in the i-th mode. Combining (2.21) and (2.22) in order to eliminate F_i, we can get six simultaneous equations which are

$$m\dot{u}_i + \dot{u}_j m_{ij} = -u_j \frac{dm_{ij}}{dt} + R_i + F_{ei} \qquad (2.23)$$

After using the usual matrix operations to solve the six simultaneous equations, the only unknowns, $\dot{u}_j$, in (2.23) are found and the hydrodynamic forces are computed by (2.21).

If the velocity potential and the fluid velocity can be evaluated without difficulty, the hydrodynamic forces and the relative positions may be calculated by performing the following steps:

1. At the current time-step, obtain the velocity potential and the fluid velocity.

2. In order to evaluate the time derivative by two-sided finite difference, move the bodies back and forth to two possible positions, and obtain the velocity potential only.

3. Solve a linear system for the unknown accelerations, and then obtain the hydrodynamic forces, if desired.

4. Move the bodies to the position of the next time-step, according the bodies' accelerations and velocities.

5. Repeat step 1 ~ step 4 for the next time-step.

Chapter 3

Solutions of the Potential Flow Problems

In order to compute the forces and moments outlined in the previous section, it is seen that the flow problems must be solved at each time-step. The flow problems are solved under the assumptions that the fluid is inviscid, and incompressible, the flow is irrotational and the free-surface effects are neglected. Then at each time-step the entire flow can be described by a velocity potential $\phi(\vec{x})$ where $\vec{x}$ is a position vector in a fixed Cartesian coordinate system (x, y, z) which is defined such that the x- and y-axes lie in the plane of the free surface and the z axis has its positive direction pointing out of the fluid domain. We use S_B to denote the surfaces of bodies, S_F the free surface, and S_C the surface which encloses the fluid. In the fluid domain which is enclosed by S_B, S_F, and S_C, the velocity potential $\phi(\vec{x})$ satisfies the Laplace's equation

$$\nabla^2 \phi = 0. \tag{3.1}$$

Boundary conditions must be provided on the surface $S_B \cup S_C \cup S_F$, with the generalized unit normal vector $\vec{n}$. On the free surface the velocity potential $\phi(\vec{x})$ satisfies the "rigid lid" boundary condition

$$\frac{\partial \phi}{\partial z} = 0 \quad on \ S_F, \tag{3.2}$$

on the enclosing boundary the velocity potential $\phi(\vec{x})$ satisfies the boundary conditions

$$\frac{\partial \phi}{\partial n} = 0 \quad on \ S_C, \tag{3.3}$$

and on any moving body surface S_B the velocity potential $\phi(\vec{x})$ satisfies the boundary conditions

$$\frac{\partial \phi}{\partial n} = \vec{U} \cdot \vec{n} \quad on \ S_B, \tag{3.4}$$

where $\vec{U}$ denotes the bodies' translational and angular velocities and $\vec{n}$ denotes the generalized normal vector.

The above boundary value problem can be solved by applying Green's theorem. Defining the field point $\vec{x} = (x, y, z)$ and the source point $\vec{\xi} = (\xi, \eta, \zeta)$, the Green function may be chosen in the following form

$$G(\vec{x}; \vec{\xi}) = \frac{1}{r} + \frac{1}{r'}, \tag{3.5}$$

where

$$r = [(x - \xi)^2 + (y - \eta)^2 + (z - \zeta)^2]^{\frac{1}{2}} \tag{3.6}$$

$$r' = [(x - \xi)^2 + (y - \eta)^2 + (z + \zeta)^2]^{\frac{1}{2}}. \tag{3.7}$$

Applying Green's theorem gives the potential formulation.

$$2\pi\phi(\vec{x}) + \int\int_{S_B \cup S_C} \phi(\vec{\xi}) \frac{\partial}{\partial n_\xi} G(\vec{x}; \vec{\xi}) dS_\xi = \int\int_{S_B \cup S_C} G(\vec{x}; \vec{\xi}) \frac{\partial}{\partial n_\xi} \phi(\vec{\xi}) dS_\xi. \tag{3.8}$$

In the potential formulation Green's theorem is used directly, with the source strength equal to the known normal velocity and the dipole moment equal to the unknown

potential. This second-kind Fredholm integral equation can then be solved for the unknown velocity potential on the body. If we represent the velocity potential by sources alone, with unknown strength $\sigma(\vec{x})$, evaluating the normal derivative on the body leads a similar Fredholm equation for the source strength.

$$2\pi\sigma(\vec{x}) + \int\int_{S_B \cup S_C} \sigma(\vec{\xi})\frac{\partial}{\partial n_x}G(\vec{x};\vec{\xi})dS_\xi = \vec{U} \cdot \vec{n}(x) \quad \vec{x} \in S_B \cup S_C. \tag{3.9}$$

From which, the fluid velocity is given by

$$\nabla\phi(\vec{x}) = 2\pi\vec{x}(x)\sigma(\vec{x}) + \int\int_{S_B \cup S_C} \sigma(\vec{\xi})\nabla_{\vec{x}}G(\vec{x};\vec{\xi})dS_\xi. \tag{3.10}$$

If S_C describes an enclosing channel with a rectangular cross section, a particular Green function which satisfies (3.3) may be used to greatly reduce the computational effort (Newman,1992) [10].

Chapter 4

The Influence of the Propeller

The influence of the propeller may be included in the ship interaction simulation. The inclusion of a propeller behind the ship hull modifies the velocity potential so that the forces experienced by both ships are different from the case with no propeller. Because of the complexity of the analysis of the flow due to the presence of a propeller, we approach this problem by considering the propeller in its simplest form as an actuator disk. In the present study, only the induced velocities on the other ship by the propeller are considered, and the changes of the velocity potential by the propeller are not taken into account.

The simplest representation of an ideal propeller is as a circular disk of negligible thickness with a diameter equal to that of the propeller. Through the disk, the flow passes continuously while subjected to a constant pressure jump across the disk. The effects of a finite number of blades and the production of fluid rotation are ignored.

An actuator is really a set of counter-rotating propellers with an infinite number of blades with constant circulation over the radius. Under such an idealization, expressions are developed for the velocity induced at a radius r_c and axial position x_c by an infinite set of helical vortices uniformly distributed around the circumference of a circle of radius r_v. Because an actuator disk is a set of counter-rotating infinite bladed lifting lines, we shall replace Z concentrated vortices of unit strength with a continuous distribution with total circulation Z.

The elimination of the circumferential variation in the flow field simplifies the

problem, and Hough and Ordway (1964) were able to find a closed-form solution in terms of elliptic integrals. Their results can be computed very rapidly, as follows:

For $r_c < r_v$

$$\bar{u}_a(x_c, r_c, r_v) = \frac{Z}{4\pi}\{\frac{1}{\pi r_v \tan \beta}C_1\}$$

$$\bar{u}_t(x_c, r_c, r_v) = \frac{Z}{4\pi}\{\frac{1}{\pi r_c}C_2\}. \tag{4.1}$$

For $r_c > r_v$

$$\bar{u}_a(x_c, r_c, r_v) = \frac{Z}{4\pi}\{\frac{1}{\pi r_v \tan \beta}C_2\}$$

$$\bar{u}_t(x_c, r_c, r_v) = \frac{Z}{4\pi}\{\frac{1}{\pi r_c}C_1\}. \tag{4.2}$$

where

$$C_1 = \pi + \frac{x_c}{2\sqrt{r_c r_v}}Q_{-\frac{1}{2}}(q) + \frac{\pi}{2}\Lambda_0(s,t)$$

$$C_2 = \frac{x_c}{2\sqrt{r_c r_v}}Q_{-\frac{1}{2}}(q) - \frac{\pi}{2}\Lambda_0(s,t), \tag{4.3}$$

and

$$q = 1 + \frac{x_c^2 + (r_c - r_v)^2}{2r_c r_v}$$

$$s = sin^{-1}\{\frac{x_c}{\sqrt{x_c^2 + (r_c - r_v)^2}}\}$$

$$t = \sqrt{\frac{4r_c r_v}{x_c^2 + (r_c + r_v)^2}}. \tag{4.4}$$

$Q_{-\frac{1}{2}}$ is the Lengendre function of the second kind and half integer order, and Λ_0 is the Heumann's Lambda function.

The circulation may be computed by the equation

$$\Gamma = \pi\frac{r_v}{Z}\tan \beta(\frac{C_T}{1 + \sqrt{1 + C_T}}), \tag{4.5}$$

24

where C_T is the thrust coefficient and β is the disturbed pitch angle.

The resultant induced velocity by the propeller is the product of the circulation and the results form the expressions above. It should be noted that the propeller coordinate system is different the body coordinate system. More description and explanation for the propeller and the actuator disk may be found in Kerwin (1990) [4].

Chapter 5

Numerical Implementation

Since (3.8), (3.9), and (3.10) can not be solved analytically, a panel method is used to solve the flow problem at each time-step. In this method, the boundary surfaces are divided into N plane quadrilateral or triangular panels over which the strengths of the singularities are assumed to be unknown constants. At each panel, the collocation point is situated at the centroid of the panel. After discretization, the integral equation (3.8) becomes

$$2\pi\phi(\vec{x}_i) + \sum_{j=1}^{N} \phi(\vec{\xi}_j)\frac{\partial}{\partial n_{\xi_j}}G(\vec{x}_i;\vec{\xi}_j)dS_{\xi_j} = \sum_{j=1}^{N} G(\vec{x}_i;\vec{\xi}_j)\frac{\partial}{\partial n_{\xi_j}}\phi(\vec{\xi}_j)dS_{\xi_j} \quad i,j = 1,2,...,N$$

$$(5.1)$$

where N is the total number of the panels, and i,j are the panel indices. (5.1) forms a linear system:

$$\sum_{j=1}^{N} \mathbf{A}_{ij}\phi(\vec{x}_i) = \mathbf{B}_i \quad i = 1,2,...,N \qquad (5.2)$$

where $\mathbf{A}$ is an NxN influence coefficient matrix, ϕ is the unknown Nx1 matrix containing the unknown velocity potential of each panel, and $\mathbf{B}$ is a known Nx1 matrix, which is determined by the boundary condition. Since we do not have any restriction on the geometry for each body, generally speaking, $\mathbf{A}$ is a non-symmetric, full matrix. A direct or an iterative method can solve (5.2) for the unknown constants $\phi(\vec{x}_i)$. In the same manner, (3.9) can be discretized and solved for the unknown source strengths $\sigma(\vec{x})$.

For the solution of the equations of motion, the quantities should be carefully defined from the viewpoint of the coordinate system. A global Cartesian coordinate system is chosen such that the x- and y- axes lie in the plane of the free surface and z axis has its positive sense directed out of the fluid volume. The body coordinate systems are defined such that the center of waterplane of the body is the origin, the orientation of the x- axis is from the stern to the bow, and the orientation of the z axis is coincident to the orientation of the global z axis. Between the body coordinate system and the global coordinate system, the only required connections for expressing the quantities are the angles among axes if the magnitudes of all coordinate systems are equal. In a integral equation, all vector quantities should be expressed in the same coordinate system. If a scalar quantity is the product of two vectors, both vectors should be expressed in the same coordinate system which is not necessary to be equal to the coordinate system in which the other vector quantities are expressed. In (3.8), (3.9), and (3.10) the vectors are expressed in the global coordinate system, and in (2.20) the vectors are expressed in the body coordinate system. It should be noted that because in (3.10) the fluid velocities are solved in the global coordinate system, for the "transport term" in (2.20) it is necessary to transform the fluid velocities into the body coordinate system.

Because the bodies are not fixed, we need to update the positions of the bodies at each time-step, with the accelerations of bodies caused by the hydrodynamic force calculated by (2.20), after solving the potential problems.

There are two different kinds of time-steps for the calculation of the hydrodynamic forces and body motions. The primary kind of time-step we simply call the "time-step" and it controls the accuracy of body motions. The other kind of time-step we call the "sub-time-step" and it controls the accuracy of the computation of the hydrodynamic forces (2.20).

The discretized form of the time derivative term in (2.23) is given by

$$\rho u_j \frac{d}{dt} \int \int_{S_B} \phi_j n_i dS = \frac{\rho u_j \sum_{k=1}^{N} (\phi_{jk}^{t+\Delta\varepsilon} - \phi_{jk}^{t-\Delta\varepsilon}) n_{ik} A_k}{2\Delta\varepsilon}, \tag{5.3}$$

27

where $k, N, A, \Delta\varepsilon$ denote the k-th panel, the number of panels, the area of the panel, and the magnitude of the sub-time-step, and $t = M\Delta t$ where M and Δt denote the M-th time-step and the magnitude of the time-step, so ϕ_{jk} is the velocity potential on the k-th panel due to a body motion with unit velocity in the j-the mode. Because (2.23) is solved in the body coordinate system and rigid body motions are assumed, the generalized normal vectors and the surface areas of the panels will not change with respect to time.

Another linear system is formed by (2.23) for the unknown accelerations. After solving (2.23), the forces may be obtained by (2.21). The evaluated forces and added-mass coefficients may be non-dimensionalized by the appropriate combinations of water density ρ, body velocity U, and body length L. The non-dimensionalization is as follows

The added-mass:

$$m_{ij} = \frac{\tilde{m}_{ij}}{\rho L^k} \tag{5.4}$$

The forces (and moments) whether the quadratic force or the total force:

$$F_{i,j} = \frac{\tilde{F}_{ij}}{\frac{1}{2}\rho U^2 L^m}. \tag{5.5}$$

In these expressions, the tilde denotes dimensional quantities, and i, j are mode indices. In (5.4) and (5.5), $k = 3$ and $m = 2$ for $i, j = 1, 2, 3, 7, 8, 9$, $k = 5$ and $m = 4$ for $i, j = 4, 5, 6, 10, 11, 12$, and $k = 4$ and $m = 3$ for the other combinations.

After solving (2.23), the displacement is given by

$$D_i^t = u_i^t \Delta t + \frac{1}{2}\dot{u}_i^t(\Delta t)^2. \tag{5.6}$$

As mentioned in §2.3, the bodies are moved to two possible positions at each time-step. If we use subscripts, o, $+$, $-$, to respectively denote the exact position and two possible positions moved from the exact position by positive and negative velocity, those displacements are given by

$$P_+^t - P_o^t = u^t \Delta \varepsilon \tag{5.7}$$

$$P_-^t - P_o^t = -u^t \Delta \varepsilon, \tag{5.8}$$

where P and u denote the position vector and the velocity vector respectively. If the body is moved form P_+^t to $P_-^{t+\Delta t}$, we can take advantage of (5.6), (5.7), and (5.8)

$$P_-^{t+\Delta t} - P_+^t = (P_-^{t+\Delta t} - P_o^{t+\Delta t}) + (P_o^{t+\Delta t} - P_o^t) + (P_o^t - P_+^t)$$

$$= -u^{t+\Delta t} \Delta \varepsilon + u^t \Delta t + \frac{1}{2} \dot{u}^t (\Delta t)^2 - u^t \Delta \varepsilon. \tag{5.9}$$

Between $u^{t+\Delta t}$ and u^t, the relation is given by

$$u^{t+\Delta t} = u^t + \dot{u}^t \Delta t. \tag{5.10}$$

Combining (5.9) and (5.10) in order to eliminate u^t, we can get

$$P_-^{t+\Delta t} - P_+^t = -u^{t+\Delta t} \Delta \varepsilon + u^{t+\Delta t} \Delta t - \dot{u}^t (\Delta t)^2 + \frac{1}{2} \dot{u}^t (\Delta t)^2 - u^{t+\Delta t} \Delta \varepsilon + \dot{u}^t \Delta t \Delta \varepsilon$$

$$= u^{t+\Delta t} (\Delta t - 2\Delta \varepsilon) - \frac{1}{2} \dot{u}^t \Delta t (\Delta t - 2\Delta \varepsilon). \tag{5.11}$$

Observing (5.11), the two positions, P_+^t and $P_-^{t+\Delta t}$ are identical and the computation is reduced if we choose the magnitude of the sub-time-step to be equal to one half of the magnitude of the time-step.

The number of panels required to achieve the desired computational accuracy and the associated computational burden are practical issues. From the viewpoint of computational effort, set-up of the linear system and solution of the linear system are dominant compared to the other processes. Since $\mathbf{A}$ is a full matrix in (5.2), set-up of the linear system requires the evaluation of N^2 influence coefficients. Solution of the linear system requires an effort proportional to N^3 computations if a direct

method like Gaussian elimination is used. This kind of computations may be reduced by a factor of N if a suitable iterative scheme is utilized. Although both set-up of a linear system and solving a linear system require $O(N^2)$ computations, set-up of a linear system really dominates the required computations according to the numerical experiment. Therefore it is enough to only include the computations of set-up of a linear system for roughly estimating the computation effort.

Compared to performing one-sided finite difference, the computation is increased in the present method for each time-step, because bodies are moved from the current positions to two possible positions in order to perform two-sided finite difference. In two-sided finite difference, for each time-step the velocity potential and the fluid velocity are required at the current position, but only the velocity potential is required at two possible positions. If we take advantage of (5.11), the computation is reduced because the solutions at two possible positions are shared with the neighboring time-steps. Thus there are two velocity potential problems and one fluid velocity problem solved for each time-step in two-sided finite difference. In one-sided finite difference, if we choose the magnitude of the sub-time-step equal to the magnitude of the time-step, the solutions at the current position are shared with the neighboring time-steps, too. Thus there are one velocity potential problem and one fluid velocity problem solved for each time-step. If we approximately estimate the computation effort, there are $C_1 N^2$ computations for set-up of a linear system where C_1 is some constant. A velocity potential problem requires $C_1 N^2$ computations because a full matrix is set up for (3.8), and a fluid velocity problem requires $4C_1 N^2$ computations because a full matrix is set up for (3.9), and $3C_1 N^2$ computations are required for three components of the gradient of the Green's function. Therefore, there are $6C_1 N^2$ computations for each time-step in two-sided finite difference, and $5C_1 N^2$ computations for each time-step in one-sided finite difference, and the ratio of computations between two methods which is 6/5. The above estimation is made via an assumption that all matrices are done individually. Actually, when matrices are set up for a velocity potential problem and a fluid velocity problem at a current position, some computed information can be shared among entries. Reconsidering the previous estimation with that in mind

there are $C_2 N^2$ additional computations for the fluid velocity problem at the current position. Therefore the ratio becomes

$$Ratio = \frac{2C_1 + C_2}{C_1 + C_2} \qquad (5.12)$$

The ratio becomes 2/1 for the extreme case in which all required information for the fluid velocity problem can be directly obtained from the solutions of the velocity potential problem, i.e. $C_2 = 0$. C_2 may vary from 0 to $4C_1$. Therefore the reasonable ratio is between 6/5 and 2. A numerical experiment will determine the ratio based on the CPU time for two different methods.

Chapter 6

Numerical Results

6.1 Demonstration

In this section, numerical results are shown for demonstration of the modified code, an extension of the program CHANEL. First of all, the global coordinate system must be introduced clearly. Figure 6-1 shows a three-dimensional global coordinate system. In this figure, the origin of the body coordinate system of the first body is situated at $x = -0.25$, $y = 0.30$, and $z = 0.00$, and the origin of the body coordinate system of the second body is situated at $x = 0.25$, $y = 0.50$, and $z = 0.00$. Figure 6-2 shows a two-dimensional global coordinate system. In this figure, the origin of the body coordinate system of the first body is situated at $x = -1.00$, and $y = 0.30$, the origin of the body coordinate system of the second body is situated at $x = 1.00$, and $y = 0.50$, and the two channel walls are at $y = 0.00$ and $y = 0.80$ respectively.

It is adopted that the channel walls are rectangular and no external forces other than the hydrodynamic forces are present in the following examples. As the first example, we compare the efficiency of the two-side finite difference and one-sided finite difference. For simplicity, we consider the case in which a 300 panel spheroid with constant unit speed in surge passes another identical fixed spheroid. In such a case the first term in (2.20) is zero. Therefore the comparison is for the second term in (2.20) and the first term in (2.6). All dimensions are scaled by the spheroid's length. The spheroid's beam is 0.1, the center-plane of the moving spheroid is situated

at $y = 0.341$, a distance away from the "lower" channel boundary, and the fixed one is at $y = 0.565$. The total channel width is 0.8 and the channel depth is 0.068. The magnitude of the time-step is 0.10 for two-sided finite difference and it's 0.05 for one-sided finite difference. The "exact" answer is obtained by a smaller magnitude, 0.04, and a five-point finite difference operator. Because the bodies are not influenced by the hydrodynamic forces, we can use this numerical differentiation technique.

Observing the results shown in Figure 6-6, apparently the performance of two-sided finite difference is superior to that of one-sided finite difference for the accuracy of the forces. It should be noted that for the same accuracy of forces the magnitude of the time-step of one-sided finite difference is smaller than that of two-sided finite difference. Therefore by observing (5.6) one-sided finite difference is better than two-sided finite difference for movement due to a smaller magnitude of the time-step. The next step is to compare the required computational burden of two methods for one time-step. As mentioned in §5, the ratio of required computations is between 6/5 and 2. If the modified code is run on a DEC 3000/700 for the case described above, It takes 6 seconds to solve a potential problem at the possible position and 13 seconds to solve a potential problem and a fluid velocity problem at the current position. Therefore the ratio is approximately 1.46, a reasonable result in light of our estimation in §5. If we presume that the results shown in Figure 6-6 achieve the same accuracy for both methods, we can determine the ratio of the required computations of two methods for a simulation process. From Figure 6-6 the required time-steps of two-sided finite difference is one half of that of one-sided finite difference for a simulation process, but for one time-step two-sided finite difference requires 1.46 times greater computational effort than one-sided finite difference. Therefore for a simulation process we conclude that two-sided finite difference requires 72 % of the computational effort of one-sided finite difference.

The second example is to compare the "convective derivative" term in (2.4) and the "transport" term in (2.6). Consider a spheroid with constant unit velocity in surge passing a fixed one. The spheroid's beam is 0.125, and the channel's width and depth are 0.8 and 0.2 respectively. For illustration this comparison is only made

33

at one position, but for different discretizations. The cases of 432, 972, 1728, 3888 panels have been tested. The moving spheroid is situated at $x = -0.2$, and $y = 0.25$, and the fixed one is at $x = 0.0$ and $y = 0.55$. The results are shown in Figure 6-7. The horizontal axis is the inversion of the number of panels. For the surge mode, the results are identical because both equations are the same in surge. Results in Figure 6-7 look convergent in sway but not in yaw. We have investigated these results carefully, but we do not yet have an explanation for this discrepancy. We would like to derive one of these terms directly from the other, but we have been unsuccessful in this effort so far.

The third example is to consider the influence of the propeller. Consider the two same mariners in a bow-on meeting. The first ship is situated at $y = 0.3$ and moves with constant unit velocity in the x direction, and the second ship is situated at $y = 0.5$ and moves with constant negative unit velocity in the x direction. The propellers are the same for two ships. The thrust coefficient and the radius of the propeller are 0.7 and 0.02 respectively, and the propeller is set at $z = -0.04$. The channel's width and the depth are 0.8, 0.068 respectively. Because we only consider the modification of the fluid velocity by the propeller, the comparison is for the integral called the "quadratic" component in (2.20). The results shown in Figure 6-8 are for the first ship and a few time-steps for illustration. Form Figure 6-8, we can conclude that the influence of the propeller on the fluid velocity is hardly noticeable as calculated by the Hough and Ordway's expression.

6.2 Application

In the following examples the bodies are free to move under the influence of the hydrodynamic forces. In the first example, we consider a mariner passing an initially stationary body, say, a whale. The length of the mariner is 148.37 meters, and it is 15 meters for the whale. After non-dimensionalizing by the length of the mariner, the beam of the mariner is 0.14, and it is 0.02 for the whale. Consider that the mariner is travelling with an initial unit velocity in an unbounded fluid but with finite depth, 0.0871. Initially, the mariner is situated at $x = -2.0$, and $y = 0.00$, and the whale is situated at $x = 0.0$, and $y = 0.07$. In other words, half of the whale is situated inside the track of the mariner. The results shown in Figure 6-9 are the forces on the whales in the global coordinate system. The horizontal axis denotes the x coordinates of the mariner. From Figure 6-9, first a positive force in the y direction pulls the whale away from the track. Therefore when the mariner approaches the whale, the whale has already been moved outside the track. Figure 6-10 shows the relative positions of the mariner and the whale at different time instants, and Figure 6-11 shows the positions of the whale only.

The second example is to consider that two mariners is in a bow-on meeting with the rectangular channel walls. The width and the depth of the channel is 0.8 and 0.068 respectively. The first ship is situated at $x = -2.0$, and $y = 0.30$, and it is $x = 2.0$, and $y = 0.50$ for the second ship. In this example, during the whole simulation both ships are subjected to given external forces equal to the initial suction forces due to the channel walls with one more minus sign. In other words, with these external forces the ship will travel straight if there is no other ship. The results shown in Figure 6-12 are the hydrodynamic forces on the first ship in the body coordinate system. The initial negative force in sway is due to the suction effects of the channel walls. Similarly, the first ship is subjected to a negative interaction force pulling the first ship away from the second ship at the beginning. Figure 6-13 shows the trajectories of the origins of the body coordinate systems of two ships respectively.

The last example is to consider that two mariners are in a bow-on meeting in an

35

unbounded fluid with finite depth, 0.0871. The first ship is situated at $x = -2.0$, and $y = 0.00$, and it is $x = 2.0$, and $y = 0.14$ for the second ship. The results shown in Figure 6-14 are the hydrodynamic forces on the first body in the body coordinate system. The pattern is similar to the previous two examples. Figure 6-15 shows the trajectories of the origins of the body coordinate systems of two ships respectively.

From the examples above, we can conclude that two bodies do not absolutely conflict when they are operating near to each other. Initially, the repulsive forces start to move the bodies away from each other. Later, the stronger attractive forces can not immediately overcome the inertia imparted by the initial repulsive forces. Therefore it is not so easy that two bodies hit each other.
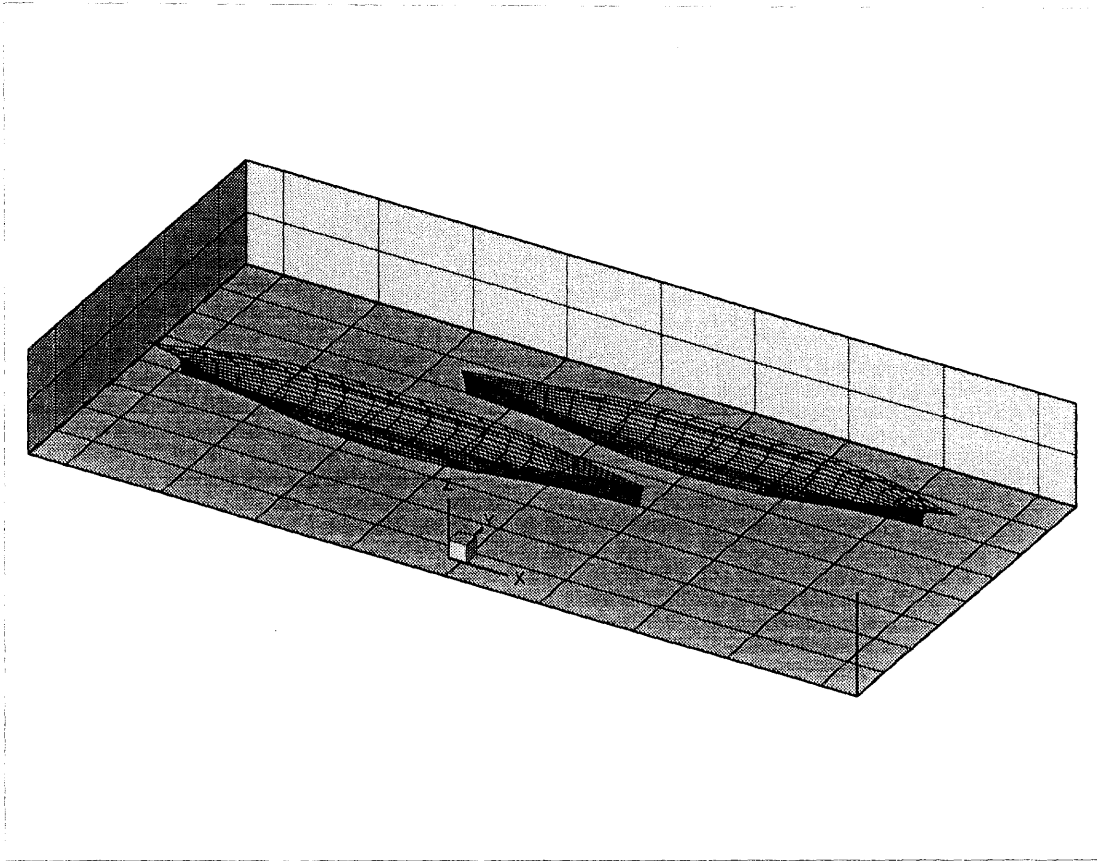
Figure 6-1: The three-dimensional global coordinate system.
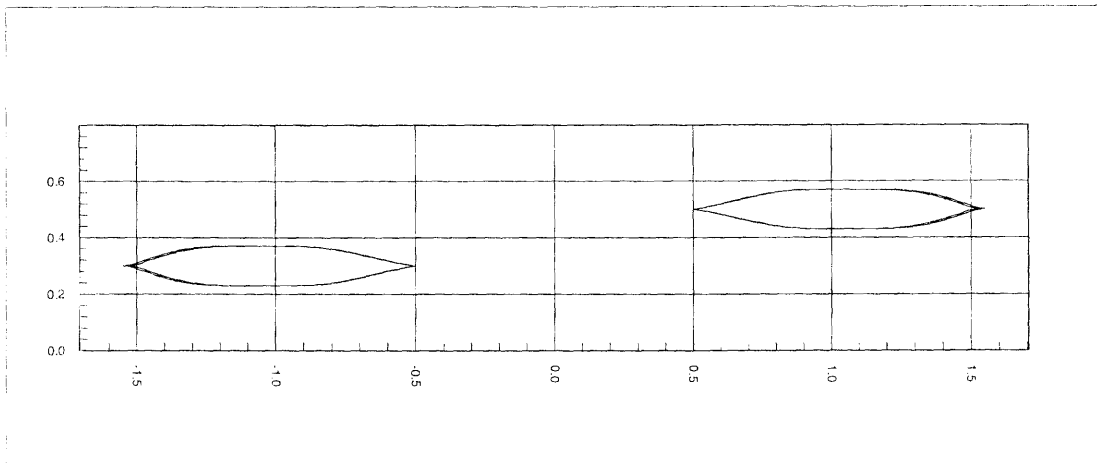
Figure 6-2: The two-dimensional global coordinate system.
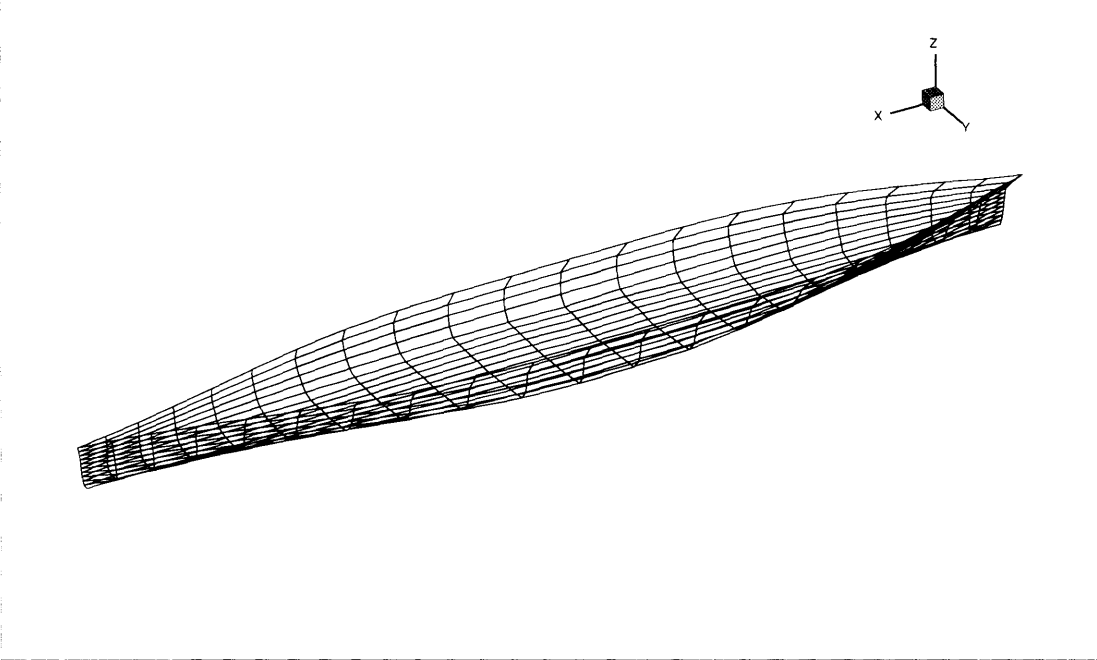
Figure 6-3: 400 panel mariner.
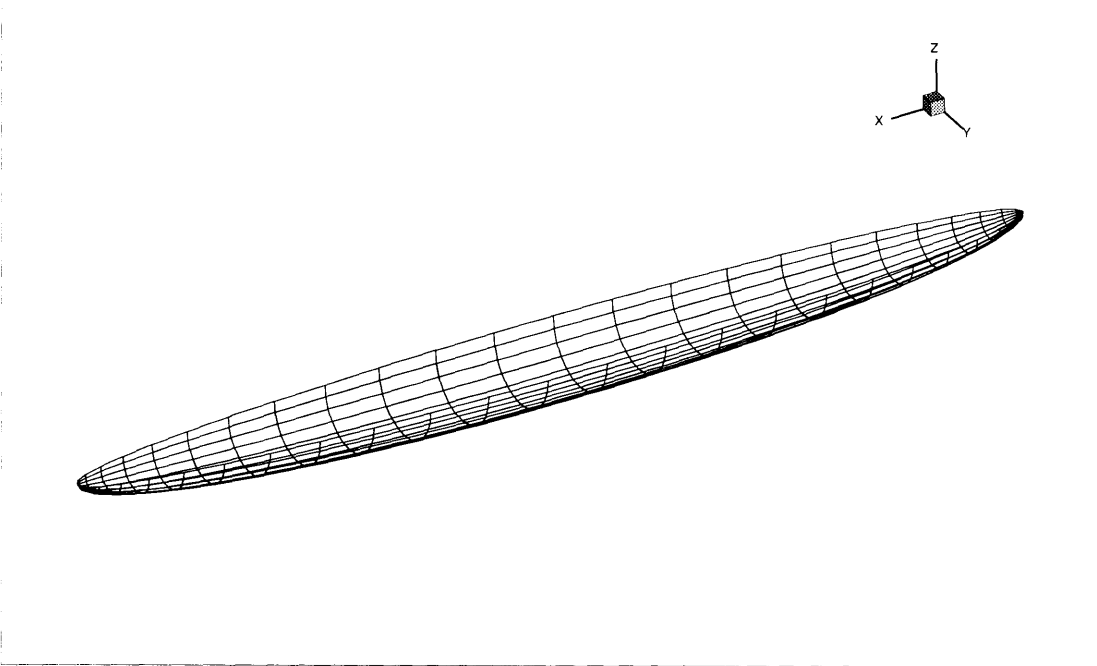
Figure 6-4: 300 panel spheroid.

38
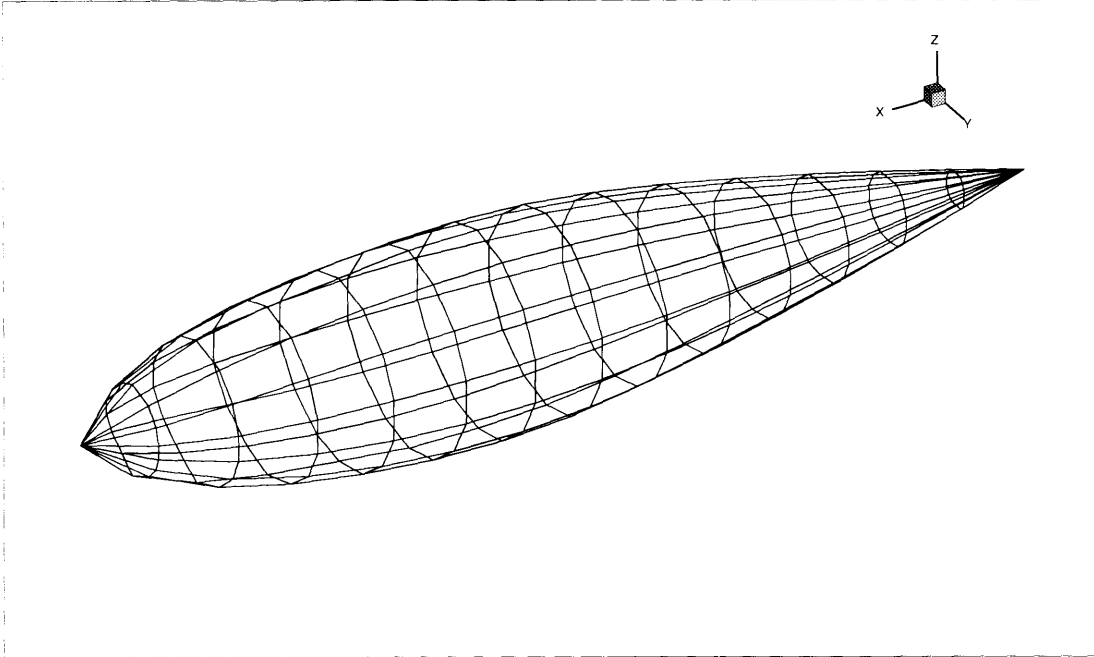
Figure 6-5: 200 panel whale.
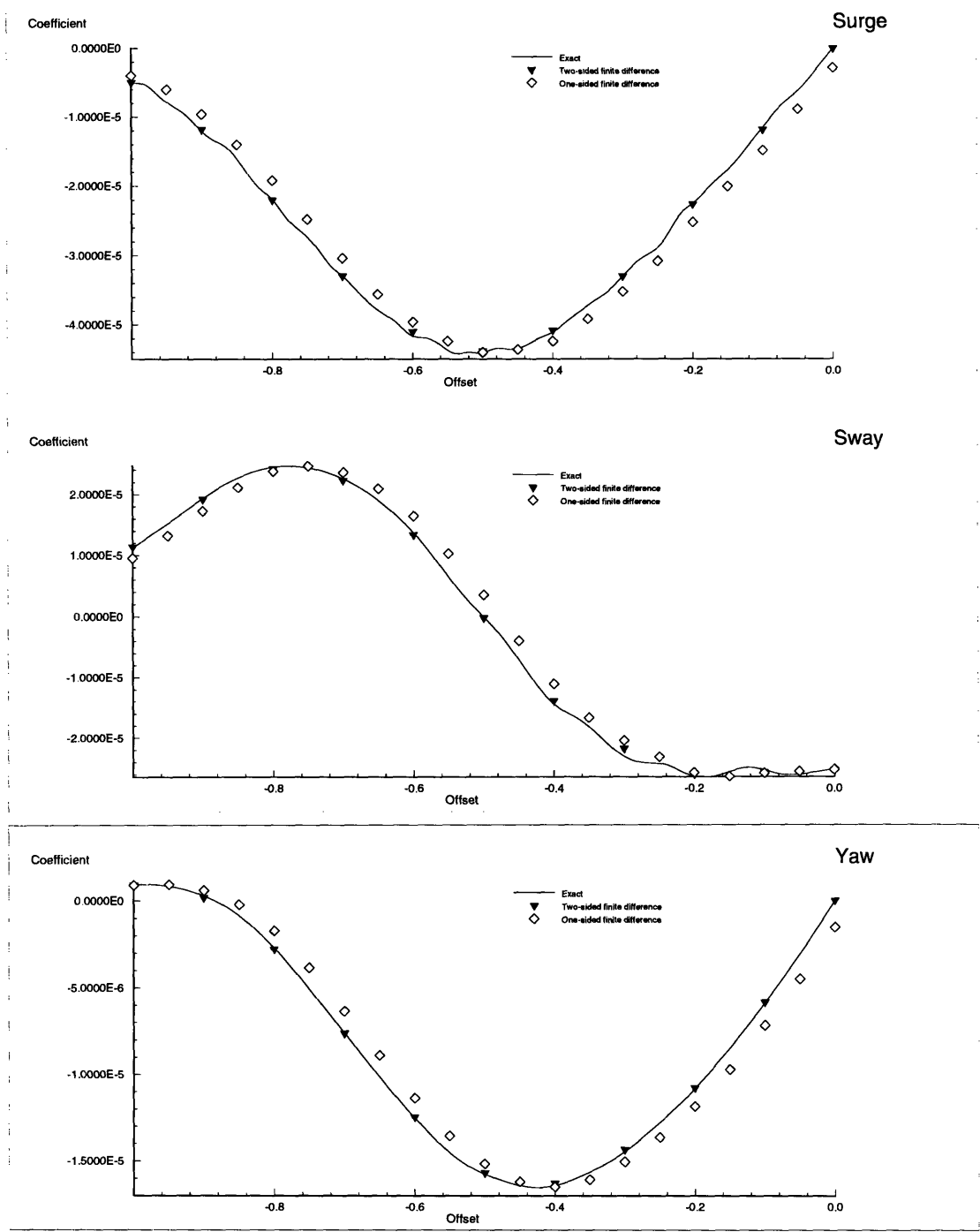
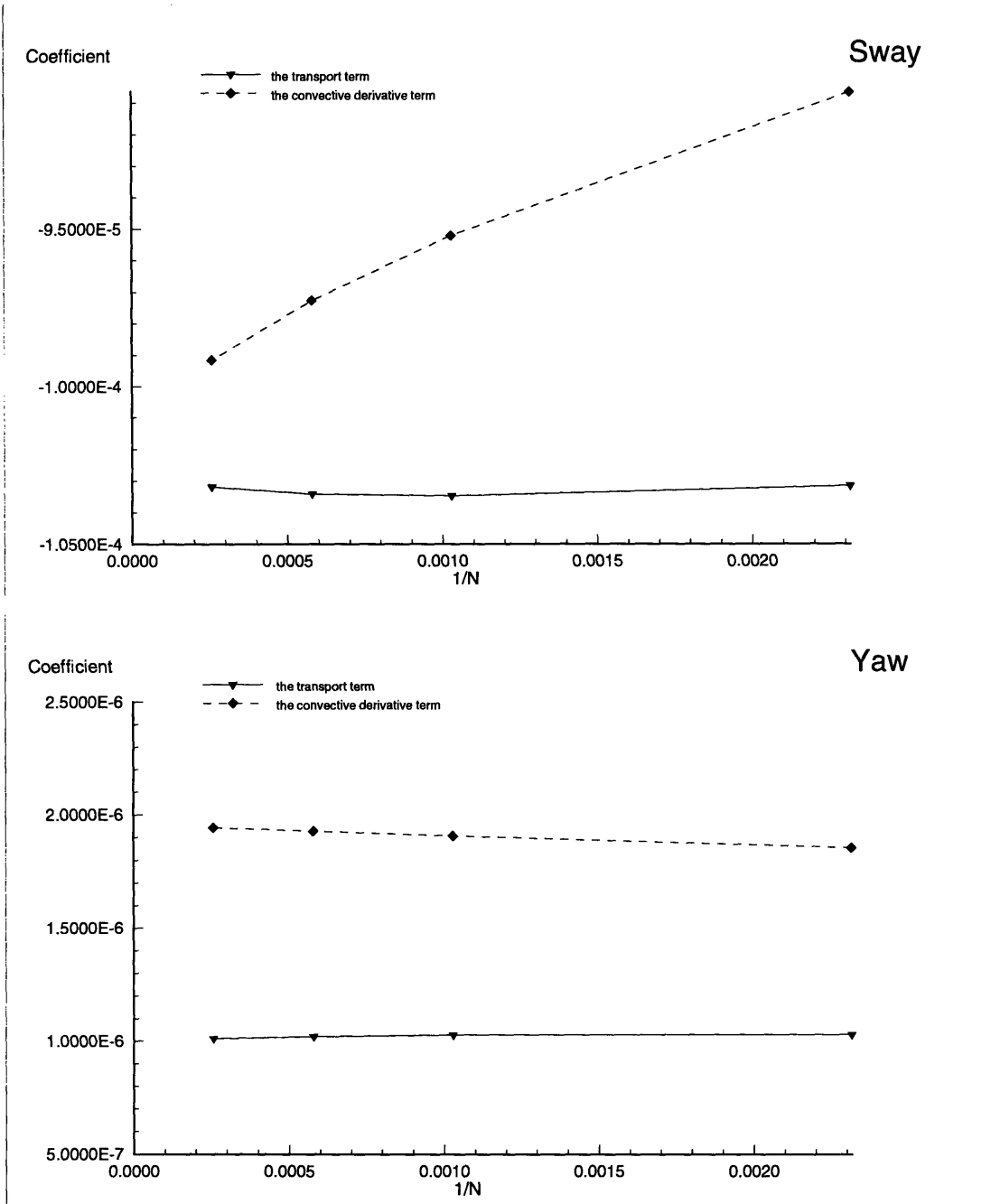Figure 6-6: Comparison of two-sided finite difference and one-sided finite difference.

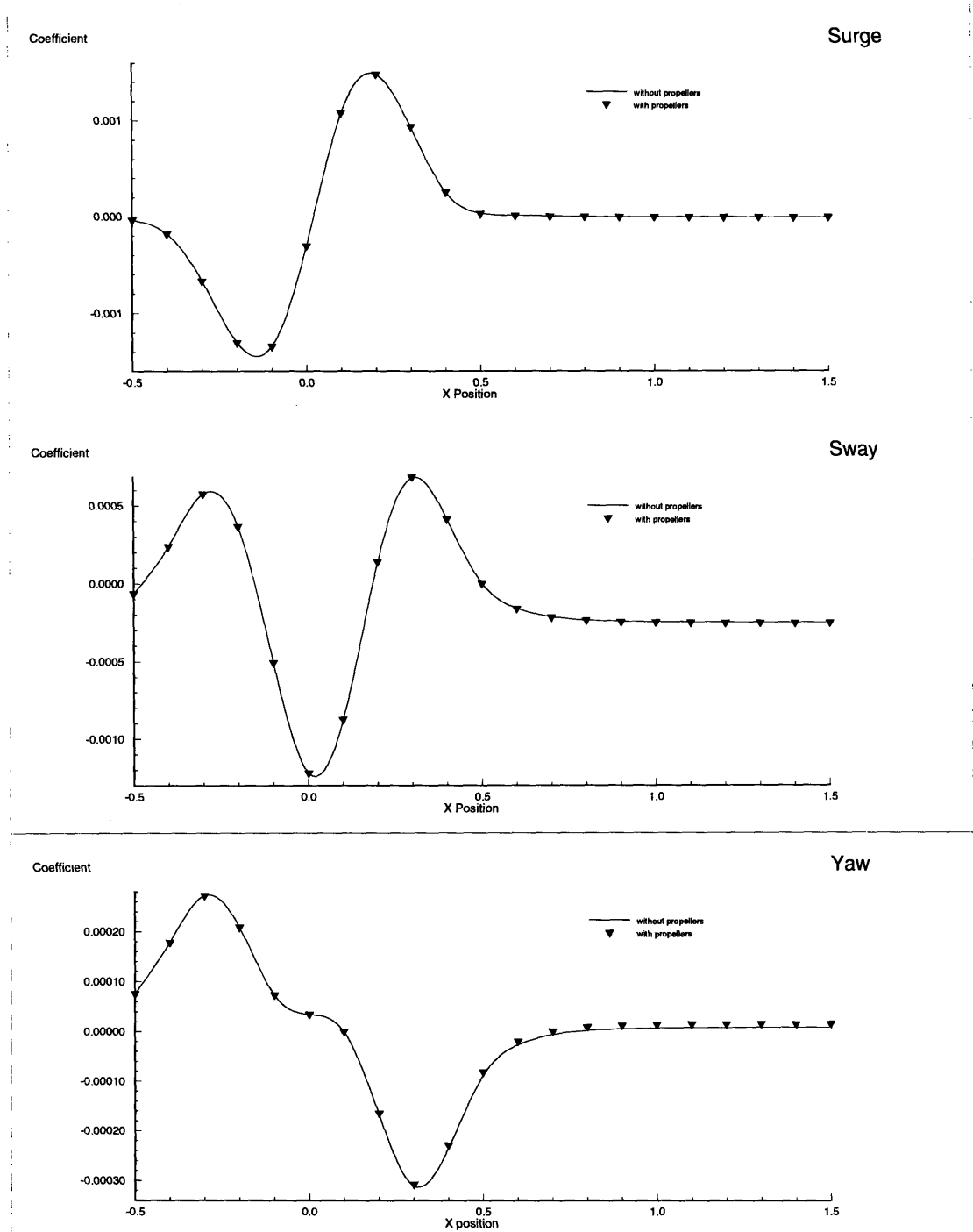Figure 6-7: Comparison of the "convective derivative" term and the "transport" term.

41

Figure 6-8: Comparison of the "quadratic" component with and without the presence of the propeller.
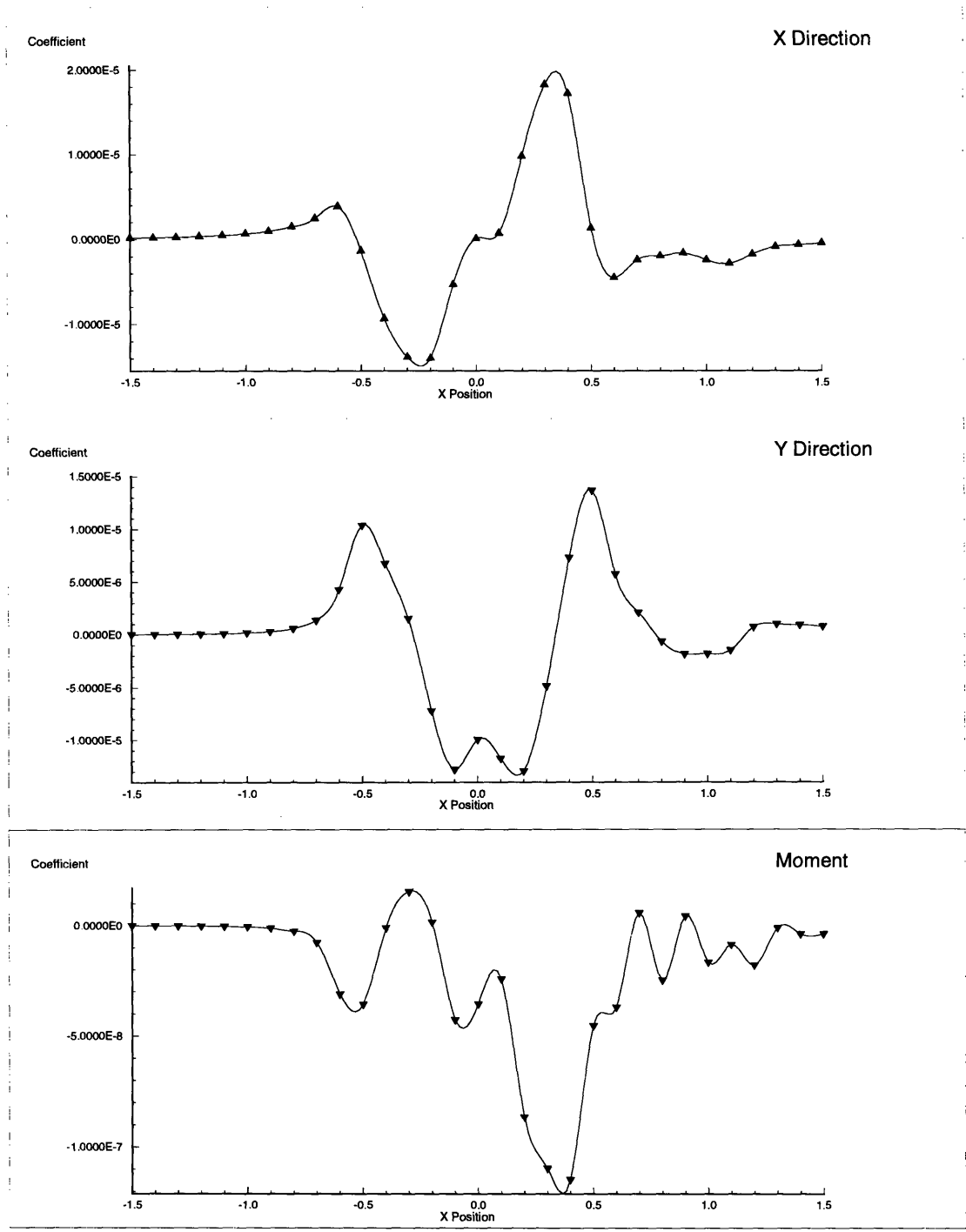
Figure 6-9: Forces on the whale in the global coordinate system.
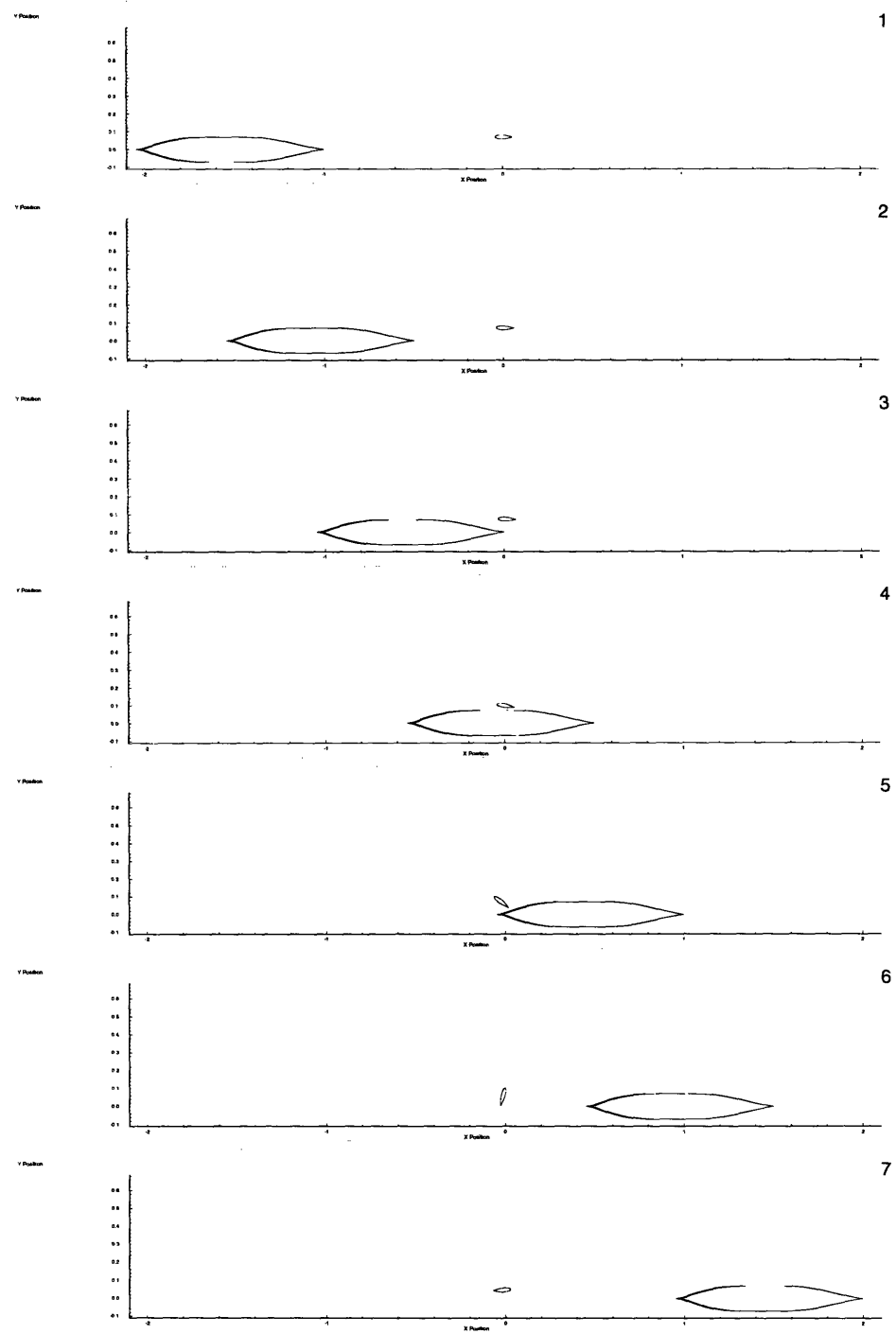
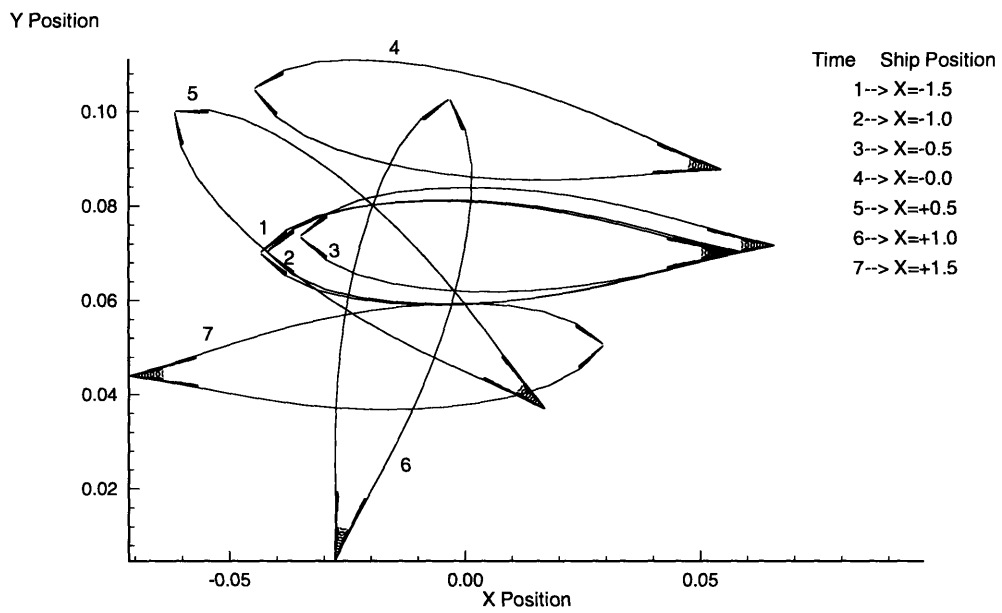Figure 6-10: Relative positions of the ship and the whale during the simulation.

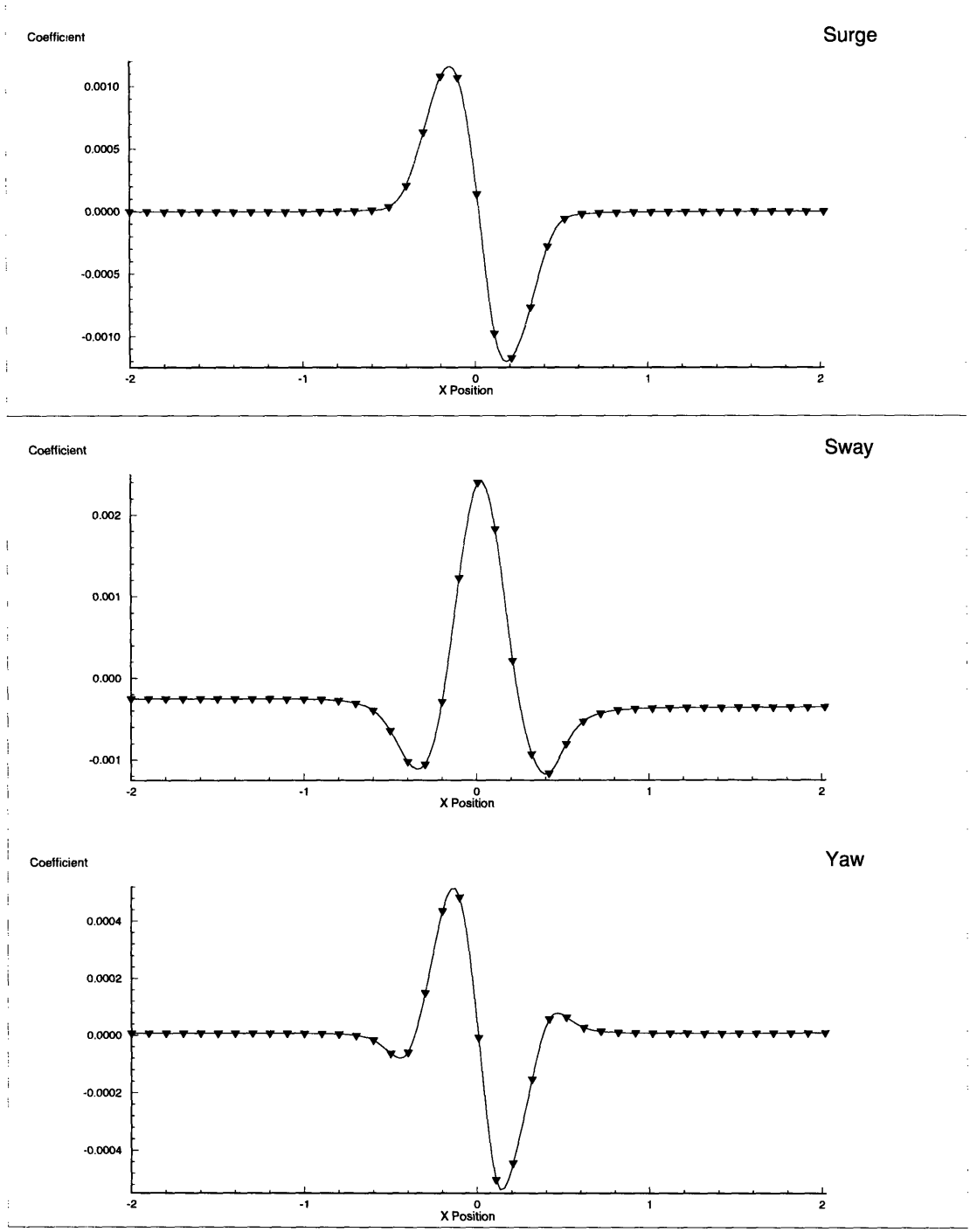Figure 6-11: The positions of the whale during the simulation.

Figure 6-12: Forces on the first ship in the body coordinate system with rectangular channel walls.
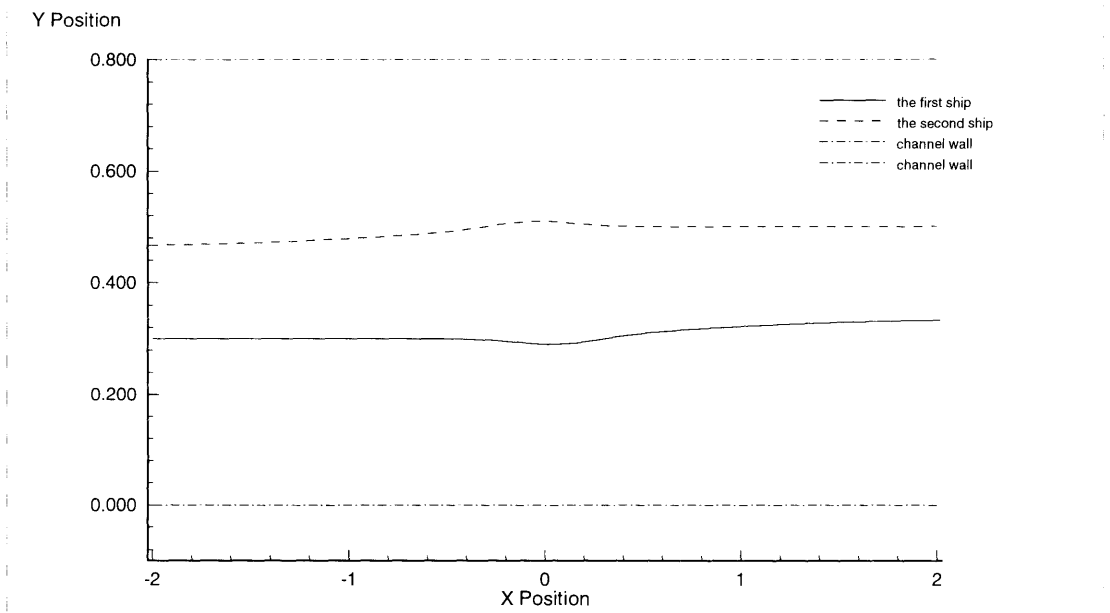
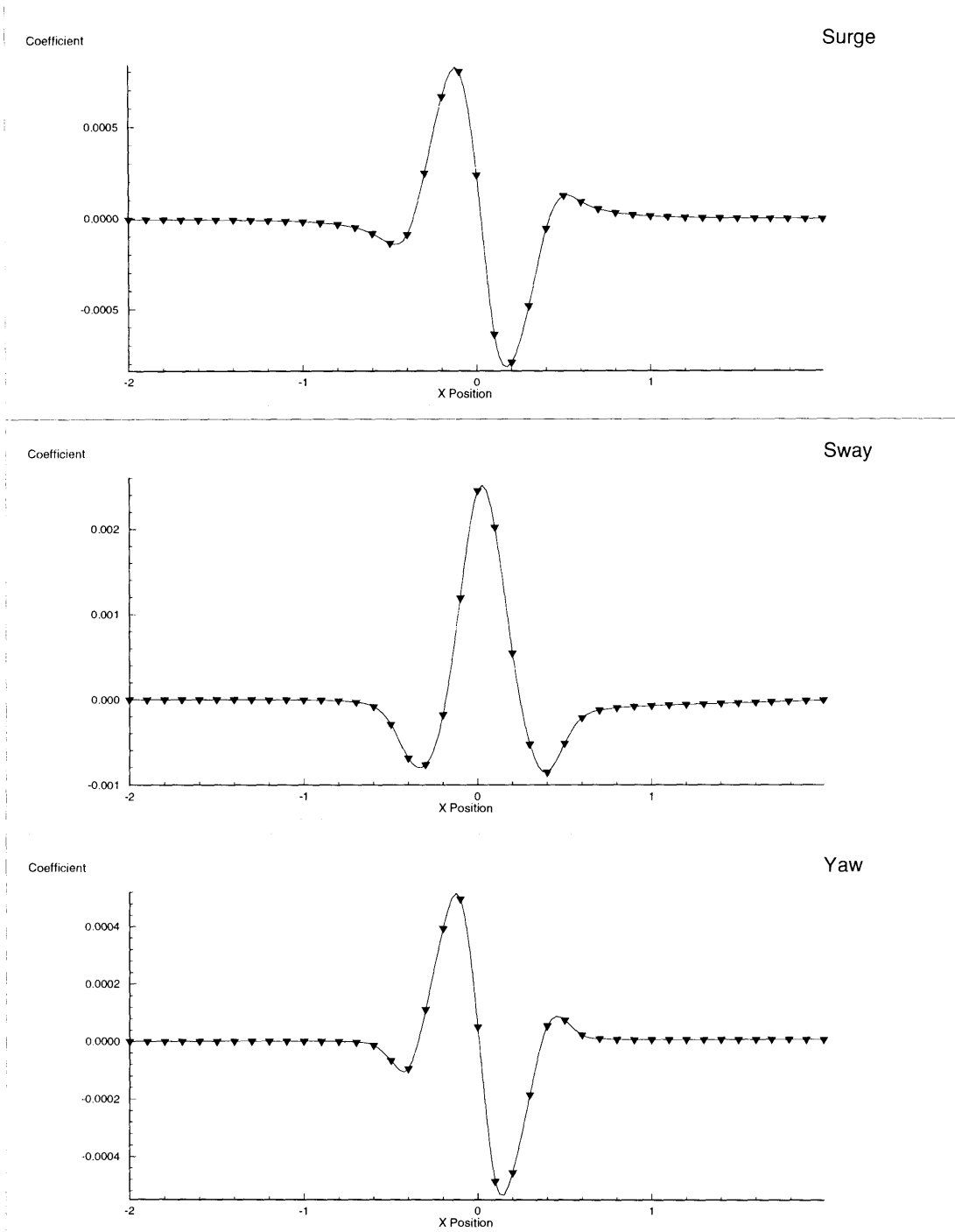Figure 6-13: The trajectories during the simulation with rectangular channel walls.

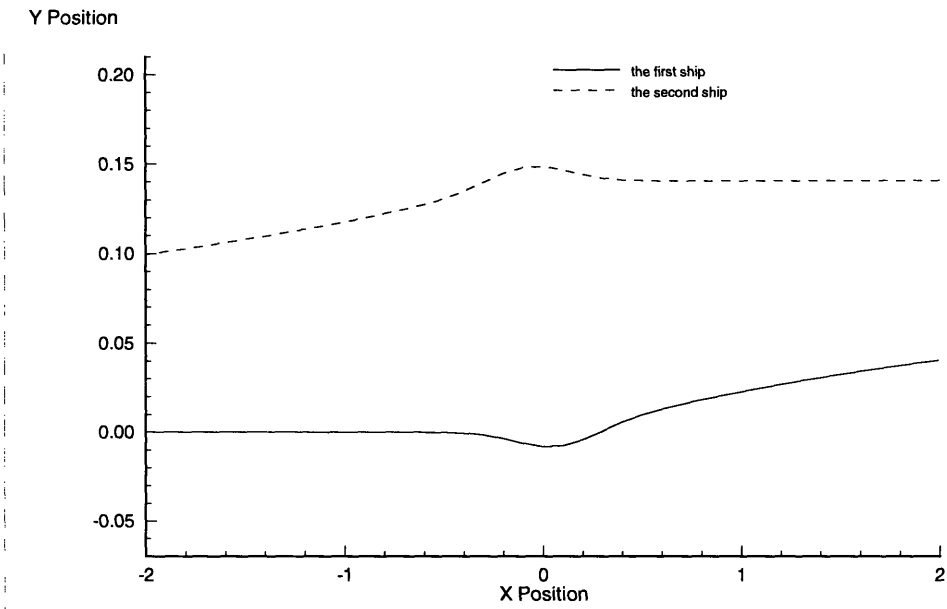Figure 6-14: Forces on the first ship in the body coordinate system.

Figure 6-15: The trajectories during the simulation.

Chapter 7

Conclusions

The present study has adopted the concept of the possible displacement for computing the time derivative term and made feasible that calculation by two-sided finite difference with consequent decreasing computations for a given accuracy. This algorithm has been utilized to predict the relative positions and the hydrodynamic forces for the cases of two bodies moved by the hydrodynamic forces.

From the results shown, we can conclude that the bodies are subjected to repulsive forces first and pushed away from each other, and later the stronger attractive forces can not immediately overcome the inertia imparted by the initial repulsive forces. Thus, the bodies do not necessarily collide when they are operating near to each other. Physically, the above description is realistic. Consider the case of a uniform flow in the x- direction past a fixed sphere. Of course, the streamlines are disturbed by the presence of the fixed sphere. Following a fluid particle just above the x- axis from minus infinity, it can be expected that the fluid particle is subjected to hydrodynamic forces and the pathline is no longer a straight one. Let's consider the motion of the fluid particle in the y- direction. The fluid particle is moved upward when it approaches the sphere, and downward when it passes the midsection of the sphere. It can be understood that the fluid particle is first subjected to a repulsive force which moves the fluid particle upward. After passing the midsection of the sphere, the fluid particle starts to move downward because the attractive force has already overcome the inertia imparted by the initial repulsive force. Therefore it can be realized that

the fluid particle is subjected to an attractive force before it passes the midsection of the sphere. The above example is more or less similar to our case of hydrodynamic interaction of bodies, if we imagine one body as a fluid particle influenced by the other body. For the case of one body moving in an unbounded fluid, the body will never run into the fluid particle because of the boundary condition. Otherwise, the fluid particle will "pierce" the body. However, the rigid body is not deformable like a mass of fluid, and two bodies could still run into each other if they are operating really close to each other.

It is still obscure to the writer that the calculations of the "convective derivative" term do not agree with those of the "transport" term. The complete connection between Lagrange's equation and Bernoulli's equation is still unsolved. We still can not directly derive the equivalence of the spatial derivatives in Lagrange's equation and the integral related to the fluid velocity in Bernoulli's equation.

Various extensions are possible. Free-surface effects can be considered by using the time-domain Green functions, and the motions in the vertical plane can be taken into account for the predictions of the motions of submarines. Rudder forces may be included in the simulation. Those extensions can extend the existing computer program to an elaborate simulator for training ship pilots.

Appendix A

Transport Theorem

The derivation of (2.5) follows from the conservation of momentum, as outlined by Newman(1977, §4.12) [9]. Before the derivation of (2.5), some preparations are required. The transport theorem is introduced,

$$\frac{dI(t)}{dt} = \int\int\int_{\mathcal{V}(t)} \frac{\partial f}{\partial t} d\mathcal{V} + \int\int_S (\vec{U} \cdot \vec{n}) f dS, \qquad (A.1)$$

where $I(t)$ is a general volume integral of the form

$$I(t) = \int\int\int_{\mathcal{V}} f(\vec{x}, t) d\mathcal{V}, \qquad (A.2)$$

where f is an arbitrary differential scalar function of position $\vec{x}$ and time t, $\mathcal{V}(t)$ is a prescribed fluid volume which may also vary with time, $\vec{x}$ is the vector containing the components of the velocities of the boundary surface, and $\vec{n}$ is the normal vector of the boundary surface. Gauss' theorem is given as

$$\int\int\int_{\mathcal{V}} \nabla f d\mathcal{V} = \int\int_S f\vec{n} dS. \qquad (A.3)$$

Let us consider that a body is surrounded by a fixed fictitious surface S_C, exterior to the body surface S_B. Thus $S_B + S_C$ forms a closed surface which encloses a fluid

volume $\mathcal{V}(t)$. Therefore, the rate of change of the fluid momentum in this volume is

$$\rho \frac{d}{dt} \int \int_{S_B + S_C} \phi \vec{n} dS = \rho \frac{d}{dt} \int \int \int_{\mathcal{V}} \nabla \phi d\mathcal{V}$$

$$= \rho \int \int \int_{\mathcal{V}} \nabla (\frac{\partial \phi}{\partial t}) d\mathcal{V} + \rho \int \int_{S_B + S_C} \nabla \phi (\mathbf{U} \cdot \vec{n}) dS$$

$$= \rho \int \int_{S_B + S_C} [\frac{\partial \phi}{\partial t} \vec{n} + \nabla \phi (\vec{U} \cdot \vec{n})] dS, \qquad (A.4)$$

where Gauss' theorem and the transport theorem have been used, and the partial time-derivative and the spatial derivative can be interchanged. Separate integrals in (A.4) over the surfaces S_B and S_C respectively with the result

$$\rho \frac{d}{dt} \int \int_{S_B} \phi \vec{n} dS + \rho \frac{d}{dt} \int \int_{S_C} \phi \vec{n} dS$$

$$= \rho \int \int_{S_B} [\frac{\partial \phi}{\partial t} \vec{n} + \nabla \phi (\vec{U} \cdot \vec{n})] dS + \rho \int \int_{S_C} (\frac{\partial \phi}{\partial t}) \vec{n} dS + \rho \int \int_{S_C} \nabla \phi (\vec{U} \cdot \vec{n}) dS. \quad (A.5)$$

The last integral is zero in (A.5) due to the boundary condition on the fixed fictitious surface S_C, $\vec{U} \cdot \vec{n} = 0$. Furthermore, $\partial \phi / \partial t = d\phi / dt$ on the fixed fictitious surface, and time-derivative and the surface integration can be interchanged. Therefore, in (A.5) the second integral on the left-hand-side equal to the second integral on the right-hand-side together with the boundary condition on the body surface S_B, $\vec{U} \cdot \vec{n} = \partial \phi / \partial n$ yield the result

$$\rho \frac{d}{dt} \int \int_{S_B} \phi \vec{n} dS = \rho \int \int_{S_B} (\frac{\partial \phi}{\partial t} \vec{n} + \frac{\partial \phi}{\partial n} \nabla \phi) dS, \qquad (A.6)$$

which is (2.5).

For a multi-body problem with channel walls, (A.6) is still valid provided that we individually apply (A.6) on each single body with the fixed fictitious surface enclosing that single body only.

53

Bibliography

[1] S.B. Cohen and R.F. Beck. Experimental and theoretical hydrodynamic forces on a mathematical model in confined waters. *Journal of Ship Research, Vol 27, No.2*, 1983.

[2] J.L. Hess and A.M.O. Smith. Calculation of nonlifting potential flow about arbitrary three-dimensional bodies. *Journal of Ship Research, Vol 6*, 1964.

[3] M. Isaacson and K.T. Cheung. Hydrodynamics of ice mass near large offshore structure. *Journal of Waterway, Port, Costal, and Ocean Engineering, Vol 114, No.4*, 1988.

[4] J.E. Kerwin. *Hydrofoils and Propellers*, chapter 8. Lecture notes, 1991.

[5] F.T. Korsmeyer, C.-H. Lee, and J.N. Newman. The computation of ship interaction forces in restricted waters. *Journal of Ship Research*, 1993.

[6] H. Lamb. *Hydrodynamics*, chapter 6. Cambridge University Press, U.K., (Sixth Edition), 1932.

[7] L. Landweber, A.T. Chwang, and Z. Guo. Interaction between two bodies translating in an inviscid fluid. *Journal of Ship Research, Vol 35, No.1*, 1991.

[8] L.M. Miline-Thomson. *Theoretical Hydrodynamics*, chapter 17.60. Macmillan, New York (Forth Edition), 1960.

[9] J.N. Newman. *Marine Hydrodynamics*, chapter 4.12. M.I.T. Press, Cambridge, 1977.

[10] J.N. Newman. The green function for a rectangular channel. *Journal of Eng. Maths.*, *Vol 6*, 1992.